To investigate the temporal relationship between the demethylation process and the acetylation process, the methylation status of the promoter region of MG63 was sequentially analyzed after exposure to MS-275 (Fig. 3D). The expression of ChM-I was gradually up-regulated in parallel with the demethylation of the promoter region in a DNA replication-dependent manner (Fig. 3D, a and b). At 120 h after the exposure to MS-275, the modification of H3-K9 was converted from dimethylation to acetylation (Fig. 3E, b), and Sp3 replaced HDAC2 (Fig. 3F, b). The expression of the ChM-I gene completely disappeared 24s hr after the withdrawal of MS-275 from the culture medium (Fig. 3D, c). At this time point, the binding of HDAC2 was restored eliminating the binding of Sp3 (Fig. 3F, c), although the promoter region was still hypomethylated (Fig. 3D, c). The methylation of CpG was gradually increased in a DNA replication-dependent manner and returned to the original status at 120 h after the withdrawal of MS-275 (Fig. 3D, d). These results suggested that MS-275 inhibited the maintenance of CpG methylation after DNA replication by replacing methylated H3-K9 with acetylated H3-K9.

Discussion

Both histone deacetylation and DNA methylation are important mechanisms to silence the transcription of genes unrelated to the biological phenotype of each cell. Acetylation of the histone tail is catalyzed by histone acetyltransferase (HAT) and analyzed using HDAC, each of which consists of a large family [4]. The acetylation status of histone associated with each genomic locus will be determined by the balance of two factors, HAT and HDAC, in each case, and therefore the deacetylation is regarded as a reversible silencing mechanism [4]. On the other hand, because there are no intrinsic factors with demethylase activity, DNA methylation catalyzed by DNA methyltransferase has been considered an irreversible silencing mechanism [3]. Recent reports have shown that these two mechanisms were not independent and moreover, closely related to each other [8–10].

One of the most intriguing results of this study is that the methylation of CpG was reduced by HDACi without further treatment with 5-Aza-dC. The reduction in methylation by HDACi seems to be dependent on DNA-replication (Fig. 3C). Several reports have emphasized the interplay between DNA methylation and histone methylation [11,12], notably, that H3-K9 dimethylation directry and H3-K9 acetylation inversely correlates with DNA methylation [5]. Loss-of-function mutations in H3-K9 methyltransferases of *Neurospora* and *Arabidopsis* were found to reduce overall levels of DNA methylation in vivo [8]. Consistent with these findings in fungi and plants, we here showed that the reduction in level of dimethylated histone H3-K9 was associated a reduction of DNA methylation at a specific residue in the regulatory region of a human gene, presumably due to the increase in acetylated histone H3-K9 caused by HDACi. The demethylating effect of another HDACi has been reported [9,10]. Further analysis of this intriguing matter may provide new insight into the regulation of gene expression by chromatin remodeling factors.

Hypermethylation of CpG dinucleotides in the core promoter region was a common feature of the three ChM-I-negative OS cell lines, which also shared deacetylation of the histone tail associated with the promoter region. The response to DNA-demethylating or histone-acetylating treatment was, however, quite different. In the case of TAKAO and Saos2, HDACi treatment failed to induce histone acetylation and therefore Sp3 binding, whereas 5-Aza-dC treatment induced Sp3 binding without modifying of histone acetylation, suggesting that DNA methylation may be a dominant factor in these cells. In the case of MG63, however, HDACi effectively induced histone acetylation and Sp3 binding in association with DNA demethylation. We have no clear explanation for the difference between these cell lines. MG63 is a unique cell line, in which the expression of osteogenic markers is not remarkable under normal culture conditions [1]. The transcription of the alkaline phosphates (ALP) gene was suppressed by CpG methylation and induced by 5-Aza-dC [13]. In contrast, 5-Aza-dC treatment failed to induce the expression of the osteocalcin and ChM-I genes, even when CpG methylation was eliminated [1,13]. In contrast, TAKAO and Saos2 retained features of osteogenic cells. Saos2 has strong ALP activity without any induction, and produces abundant immature bone tissue, osteoid, in the subcutaneous environment of athymic mice (data not shown). It is intriguing whether the difference in differentiation stage relates to the difference in the plasticity of epigenetic regulation, and the ChM-I gene in OS cells will be a suitable material with which to investigate this important issue.

Acknowledgments

We are grateful for Dr. M. Nakanishi for providing helpful suggestions. This work was supported by Grants-in-Aid for Scientific Research from the Japan Society for the Promotion of Science, from the Ministry of Education, Culture, Sports, Science, and Technology, and from the Ministry of Health, Labor, and Welfare.

References

[1] T. Aoyama, T. Okamoto, S. Nagayama, K. Nishijo, T. Ishibe, K. Yasura, T. Nakayama, T. Nakamura, J. Toguchida, Methylation in the core-promoter region of the chondromodulin-I gene determines the cell-specific expression by regulating the binding of transcriptional activator Sp3, J. Biol. Chem. 279 (2004) 28789–28797.

[2] Y. Hiraki, H. Tanaka, H. Inoue, J. Kondo, A. Kamizono, F. Suzuki, Molecular cloning of a new class of cartilage-specific matrix, chondromodulin-I, which stimulates growth of cultured chondrocytes, Biochem. Biophys. Res. Commun. 175 (1991) 971–977.

[3] M. Esteller, Cancer epigenomics: DNA methylomes and histone-modification maps, Nat. Rev. Genet. 8 (2007) 286–298.

[4] T. Jenuwein, C.D. Allis, Translating the histone code, Science 293 (2001) 1074–1080.
[5] Y. Kondo, L. Shen, J.P. Issa, Critical role of histone methylation in tumor suppressor gene silencing in colorectal cancer, Mol. Cell. Biol. 23 (2003) 206–215.
[6] W. Zhao, H. Soejima, K. Higashimoto, T. Nakagawachi, T. Urano, S. Kudo, S. Matsukura, S. Matsuo, K. Joh, T. Mukai, The essential role of histone H3 Lys9 di-methylation and MeCP2 binding in MGMT silencing with poor DNA methylation of the promoter CpG island, J. Biochem. (Tokyo) 137 (2005) 431–440.
[7] Q. Gan, T. Yoshida, O.G. McDonald, G.K. Owens, Concise review: epigenetic mechanisms contribute to pluripotency and cell lineage determination of embryonic stem cells, Stem Cells 25 (2007) 2–9.
[8] H. Tamaru, E.U. Selker, A histone H3 methyltransferase controls DNA methylation in Neurospora crassa, Nature 414 (2001) 277–283.
[9] N. Cervoni, M. Szyf, Demethylase activity is directed by histone acetylation, J. Biol. Chem. 276 (2001) 40778–40787.
[10] J.N. Ou, J. Torrisani, A. Unterberger, N. Provencal, K. Shikimi, M. Karimi, T.J. Ekstrom, M. Szyf, Histone deacetylase inhibitor Trichostatin A induces global and gene-specific DNA demethylation in human cancer cell lines, Biochem. Pharmacol. 73 (2007) 1297–1307.
[11] L.M. Johnson, X. Cao, S.E. Jacobsen, Inteplay between two epigenetic marks: DNA methylation and histone H3 lysine 9 methlyation, Curr. Biol. 12 (2002) 1360–1372.
[12] Y. Zhang, D. Reinberg, Transcription regulation by histone methylation: interplay between different covalent modifications of the core histone tails, Gene. Dev. 15 (2001) 2343–2360.
[13] R.M. Locklin, R.O. Oreffo, J.T. Triffitt, Modulation of osteogenic differentiation in human skeletal cells in Vitro by 5-azacytidine, Cell Biol. Int. 22 (1998) 207–215.

Available online at www.sciencedirect.com
ScienceDirect
Biochemical and Biophysical Research Communications 365 (2008) 406–412
BBRC
www.elsevier.com/locate/ybbrc

Expression of vascular cell adhesion molecule-1 indicates the differentiation potential of human bone marrow stromal cells

Kenichi Fukiage [a,b], Tomoki Aoyama [a], Kotaro R. Shibata [a,b], Seiji Otsuka [a,c], Moritoshi Furu [a,b], Yoshiki Kohno [a,b], Kinya Ito [a,c], Yonghui Jin [a], Satoshi Fujita [d], Shunsuke Fujibayashi [b], Masashi Neo [b], Tomitaka Nakayama [b], Takashi Nakamura [b], Junya Toguchida [a,*]

[a] *Department of Tissue Regeneration, Institute for Frontier Medical Sciences, Kyoto University, 53 Kawahara-cho, Shogoin, Sakyo-ku, Kyoto 606-8507, Japan*
[b] *Department of Orthopaedic Surgery, Graduate School of Medicine, Kyoto University, Japan*
[c] *Department of Musculoskeletal Medicine, Graduate School of Medical Sciences, Nagoya City University, Nagoya, Japan*
[d] *Department of Reparative Materials, Institute for Frontier Medical Sciences, Kyoto University, Japan*

Received 11 October 2007
Available online 5 November 2007

Abstract

Bone marrow stromal cells (BMSCs) are a mixture of cells differing in differentiation potential including mesenchymal stem cells, and so far no CD antigens were found to be predictable for the differentiation property of each BMSC. Here we attempted to isolate differentiation-associated CD antigens using 100 immortalized human BMSC (ihBMSC) clones. Among 13 CD antigens analyzed, only CD106/Vascular cell adhesion molecule-1 (VCAM-1) showed a clear correlation with the differentiation potential of each clone; CD106-positive ihBMSC clones were less osteogenic and more adipogenic than CD106-negative clones. This association was confirmed in primary BMSCs sorted by CD106, showing that the CD106-positive fraction contained less osteogenic and more adipogenic cells than the CD106-positive fraction. The evaluation of CD106 fraction of BMSC strains in early passages predicted clearly the osteogenic and adipogenic potential after in vitro induction of differentiation, indicating the usefulness of CD106 as a differentiation-predicting marker of BMSC.

Keywords: Bone marrow stromal cell; Cell surface marker; CD106; Adipogenesis; Osteogenesis; Mesenchymal stem cell

Mesenchymal stem cells (MSCs) are defined as plastic-adherent fibroblastic cells with the potential to differentiate into multiple mesenchymal tissues, including bone, cartilage, and fat [1]. There have been many reports of regeneration therapy using bone marrow stromal cells (BMSCs), which are heterogeneous cell populations including MSCs [2,3]. One long-standing enigma concerning MSCs is whether they have a specific cell surface marker such as the CD34 in hematopoietic stem cells. A number of CD antigens and other cell surface molecules have been proposed as candidates and attempts have been made to concentrate MSC populations using such markers by cell sorting techniques. STRO-1 is one classical candidate for an MSC-related cell surface marker, and the fraction of BMSCs sorted with anti-STRO-1 antibody was shown to be rich in MSC-like cells [4]. CD105/endoglin, formerly known as SH2, is also used as an MSC-associated marker to evaluate the efficacy of isolation procedures [5]. Recently, low affinity nerve growth factor receptor (LNGFR) has been proposed as an MSC-associated marker. $LNGFR^+$ mononuclear cells from bone marrow were rich in clonogenic precursors and differentiated into multiple lineages [6]. The modulation of antigen expression was analyzed until the 10th passage, and BMSCs

* Corresponding author. Fax: +81 75 751 4646.
E-mail address: togjun@frontier.kyoto-u.ac.jp (J. Toguchida).

0006-291X/$ - see front matter © 2007 Elsevier Inc. All rights reserved.
doi:10.1016/j.bbrc.2007.10.149

retained high levels of CD29, CD44, CD90, and CD105 [7]. Expression of CD106 and CD166 was lost gradually through long-term culture [7,8]. $CD106^+$ cells in bone marrow also demonstrated high clonogeneity and the potential to differentiate in potential to differentiate in multiple directions [9].

In spite of these extensive studies, no definite answer has been yet obtained. This is, at least partially, due to the heterogeneity of cell populations analyzed as MSCs. The clonal analysis of BMSCs is a rational approach to identifying cell surface markers associated with multi-directional differentiation potential. This approach, however, requires a considerable number of cell divisions in vitro, which is not feasible for BMSCs with a limited growth potential. Several groups including ours have established immortalized human BMSCs (ihBMSCs) [10–12]. When analyzed as a whole, ihBMSCs demonstrated multi-directional differentiation potential encompassing osteogenic, adipogenic, and chondrogenic lineages. Clonal analyses, however, revealed that ihBMSC clones were heterogeneous in terms of differentiation potential [10]. This heterogeneity would be useful for identifying differentiation-associated cell surface markers. The identification of such markers may contribute to the clinical application of BMSCs. Most current procedures to induce differentiation into a particular lineage require considerable time. For example, the osteogenic or adipogenic differentiation potential of isolated BMSCs is not known until 2 weeks after the induction of differentiation. This can cause serious problems if the quality turns out to be not good enough for use. Therefore, it would be useful for regeneration therapy using BMSCs to have markers with which to predict the differentiation potential of isolated BMSCs before the induction of differentiation.

Here we addressed this issue using clonal ihBMSCs established through the introduction of hTERT and Bmi1 genes [13], because the karyotype of this cell line is near diploid with less chromosomal aberrations than the ihBMSCs established with hTERT and HPVE6E7 [11,13]. Then, we clarified the relationship between CD106/VCAM-1 expression and differentiation potential of BMSC.

Materials and methods

Cells and tissue samples

ihBMSCs were established by sequential transduction of the hTERT and Bmi1 genes [13], and cultured in Dulbecco's modified Eagle's medium (DMEM, Sigma–Aldrich, St. Louis, MI) with 10% fetal bovine serum (FBS, Hyclone, South Logan, UT). Subcloning of ihBMSCs was performed by limited dilution, and 100 clones were established and cultured under the same conditions.

Primary human BMSCs (designated as huBM) were isolated from the bone marrow taken from iliac crests of donors, who received orthopedic operative procedures, and cultured by means of a previously described method [14,15]. Briefly, mononuclear cells were isolated from the bone marrow aspirates by density centrifugation, and then washed twice, and suspended in DMEM supplemented with 10% FBS. All procedures were approved by the Ethics Committee of the Faculty of Medicine, Kyoto University, Japan, and informed consent was obtained from each donor.

Differentiation procedures and qualitative and quantitative evaluation

Adipogenic differentiation. Adipogenic differentiation induction was performed by the standard method described previously [14]. Cells were then fixed in 10% buffered formalin and stained with 0.3% Oil-Red-O (Nacalai Tesque, Kyoto, Japan). Clones were categorized as adipogenic when Oil-Red-O positive mature lipoblasts were found in the dish regardless of the number. To quantify the differentiation potential, cells were lysed in 0.1% Thesit (Fluka Chemika, Buchs, Switzerland), and then triglyceride (TG) amounts in the cells were quantified by serum triglyceride determination kit (Sigma–Aldrich). For same samples, protein amounts were quantified using BCA protein assay reagent (Pierce Biotechnology, Rockford, IL). The assays were performed according to the manufacturer's directions.

Osteogenic differentiation. Osteogenic differentiation induction was performed by the standard method described previously [14]. To visualize calcium deposits, cultures were fixed in 100% ethanol (Nakalai Tesque), and stained with 1% Alizarin-Red (Waldeck GmbH&Co, Muenster, Germany). Clones were categorized as osteogenic when Alizarin-Red positive nodules were found in the dish regardless of the number. Alkalinephosphatase (ALP) staining was performed by a method previously described [16]. ALP activity was measured with a Phosphate Substrate kit (BioRad, Hercules, CA). Amounts of DNA were also quantified by PicoGreen dsDNA Quantitation kit (Invitrogen, Carlsbad, CA). The assays were performed according to the manufacturer's directions.

Chondrogenic differentiation. Chondrogenic differentiation induction was performed by the standard method described previously [14]. Cryosections were stained with Alcian blue (Muto Pure Chemicals, Tokyo, Japan). Clones were categorized as chodrogenic when an Alcian blue-positive matrix was found in the pellet regardless of the amount. Glycosaminoglycan (GAG) contents in the pellets were quantified by BLYSCAN Dye and Dissociation reagents (BIOCOLOR, Belfast, UK) according to manufacturer's directions. Amounts of DNA were also quantified by PicoGreen dsDNA Quantitation kit.

Reverse transcription (RT)-PCR

Total RNA was extracted from cells using an RNeasy plus mini kit (Qiagen, Hilden, Germany), and reverse-transcribed with the SuperScript III first strand system (Invitrogen). The synthesized cDNA was used as a template for each PCR, and the products were electrophoresed on 2% agarose gels and visualized by ethidium bromide staining. Information on the primer pairs is available upon request.

Complementary DNA for quantitative RT-PCR (QRT-PCR) was synthesized by the same method as above. For each sample and gene, 25 μl reactions were set up in triplicate, each with 12.5 μl of Syber Green supermix (Applied Biosystems, Foster City, CA), 0.5 pmol of each primer, and 0.3 μl of cDNA. The levels of the CD106 and β-actin genes were determined with an ABI Prism 7700 Sequence Detection System (Applied Biosystems) using the same primer pairs as in RT-PCR.

Flow cytometry (FCM)

PE-conjugated antibody against human VCAM-1 and PE-conjugated non-immune mouse IgG (isotype control) were purchased from BD Biosciences (BD, San Diego, CA). Before FCM, cells were trypsinized and washed in PBS with 0.5% BSA and 2 mM EDTA. The cells (1×10^5) were incubated with antibody (2 μl) or isotype control. The acquisition was performed in FACS Calibur (BD) using CellQuest software (BD).

Magnet activated cell sorting (MACS)

Trypsinized cells were washed with buffer consisting of PBS with 0.5% BSA and 2 mM EDTA. The cells (1×10^6) were incubated with 20 μl of PE-conjugated anti-human VCAM-1 antibody (BD), and then with 20 μl of anti-PE magnet beads (Miltenyi Biotec, Bergisch Gladbach, Germany). After being washed at each step, the cells were applied to the sorting

column. An MS column (Miltenyi Biotec) for positive sorting and an LD column (Miltenyi Biotec) for negative sorting were used.

Statistical analyses

Statistical analyses were performed using Statcel software. Data were assessed using the Pearson product-moment correlation coefficient and Student's *t*-test.

Results

Heterogeneous differentiation potential of ihBMSC clones

One hundred single-cell derived clones were established from the parental ihBMSC by limited dilution. No significant difference was observed among clones in terms of growth potential (data not shown). The adipogenic, osteogenic, and chondrogenic potential of each clone was determined by the standard induction method and categorized as either positive or negative based on the definition described in Materials and methods section. Five clones showed tri-directional differentiation, and 78 clones showed the potential to differentiate into either two or one lineage, and 17 clones showed no differentiation potential (Supplementary Table 1). This heterogeneity concerning differentiation potential was essentially the same as we previously described in ihBMSCs established with hTERT and HPVE6E7 [10].

Expression of CD106 correlated with the differentiation property of immortalized clones

The expression of 13 CD antigens, among which 10 were known to be positive in hMSC and three were negative [17,18], in 100 clones was analyzed by RT-PCR using gene specific primers (Supplementary Fig. 1). All three MSC-negative antigens were negative or only weakly positive and all 10 MSC-positive antigens were positive in all clones except CD10 and CD106. The expression of CD10 and CD106 was positive in 65 and 35 clones, respectively. There was no clear association between the expression of CD10 and any of the three differentiation potentials. But, the expression of CD106 showed an association with the differentiation potential of ihBMSC clones, especially with osteogenic differentiation potential (Fig. 1A). Then the expression level of CD106 in each clone was evaluated by QRT-PCR. CD106 expression negatively correlated with the osteogenic differentiation potential ($P < 0.01$, Fig. 1B). In case of adipogenic differentiation the expression of CD106 was higher in clones with differentiation

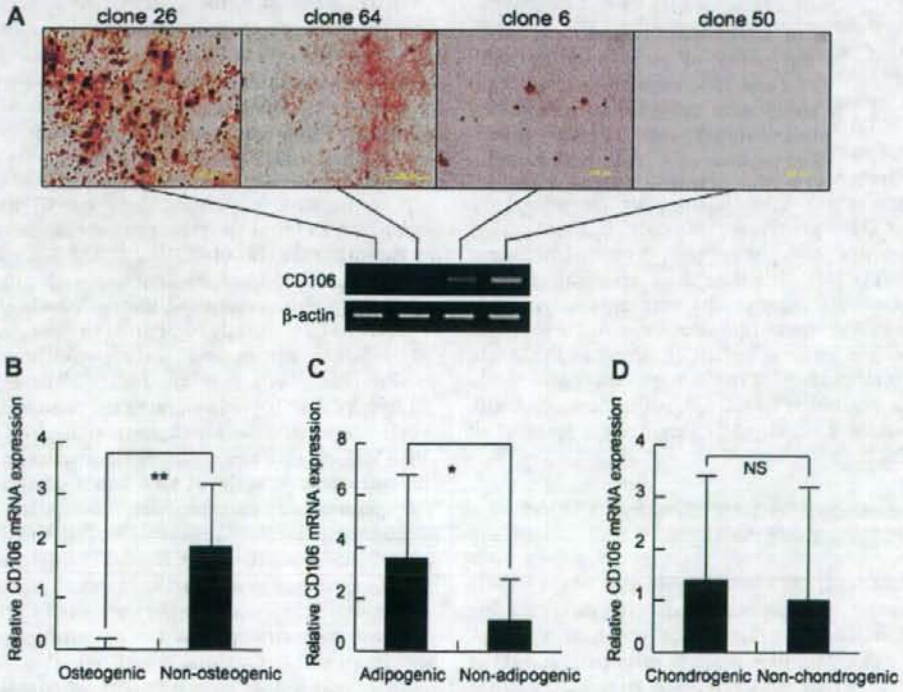

Fig. 1. The expression of CD106 correlated with the differentiation potential in ihBMSC clones. (A) Alizarin-Red staining and the mRNA expression of the CD106 gene in 4 representative clones that differ in osteogenic potential. The mRNA expression of the CD106 relative to the control gene (β-actin) was quantified by QRT-PCR in (B–D). (B) The average expression of CD106 in 29 osteogenic ihBMSC clones was significantly weaker than that in 71 non-osteogenic clones (**$P < 0.01$). (C) The average expression of CD106 in 46 adipogenic ihBMSC clones was significantly higher than that in 54 non-adipoogenic clones (*$P < 0.05$). (D) The average expression of CD106 was compared in chondrogenic and non-chondrogenic clones (NS, not significant).

potential than those without differentiation potential ($P < 0.05$, Fig. 1C), but there was no significant correlation between chondrogenic differentiation potential and the expression of CD106 in ihBMSC clones (Fig. 1D). Cell surface expression of CD106 in ihBMSC clones determined by FCM correlated with the data of QRT-PCR (data not shown). These results suggested that the ihBMSC clones positive for CD106 were less osteogenic and more adipogenic than those negative for CD106.

Expression of CD106 correlated with the differentiation property of primary BMSC

To confirm that the association of CD106 with differentiation potential was not a product of the immortalization process, the differentiation property of primary BMSC sorted by the expression of CD106 was analyzed. Both early (2nd) and late (passage 12th) cells were available for the analysis in six huBM strains. The fraction of CD106-positive cells at early passages showed a considerable difference among strains, ranging from 30% to 95% (Fig. 2A), and all strains showed a passage-dependant reduction in numbers of CD106-positive cells (Fig. 2B).

MACS was performed using antibody against CD106 in each huBM at an early passage. In the case of huBM49 at PN5, the population of CD106-positive cells was 80% before sorting, and the purity of positive-sorting and negative-sorting was 97% and 75%, respectively (Fig. 2C). When cells in each group were subjected to osteogenic induction, CD106-positive-sorted cells showed fewer number of Alizarin-Red-positive cells (data not shown), and less activity of ALP (Fig. 2D) than CD106-negative-sorted cells. On the other hand, after the adipogenic induction, CD106-positive-sorted cells included many Oil-red-O-positive cells (data not shown) and larger amounts of TG (Fig. 2E) than those of negative-sorted cells. Essentially the same results were obtained in additional three huBM strains (data not shown). These results were compatible with the results obtained in ihBMSCs, indicating that primary BMSCs were heterogeneous in terms of the expression of CD106, which correlated with the osteogenic and adipogenic differentiation potential of each BMSC.

Prediction of differentiation property based on CD106 expression in primary BMSCs

Above data suggested that the evaluation of the CD106 fraction at early passages may predict the differentiation potential of each huBM strain. As for osteogenic potential, ALP activity of each huBM strain at early passage did not correlate with the ALP activity of the corresponding huBM strain after the osteogenic induction (Fig. 3A). On the other hand, the fraction of CD106-positive cells at early passage showed a clear negative correlation with the ALP activity after osteogenic induction (Fig. 3B). The TG was almost undetectable in all huBM strains at early passage, indicating no value for the prediction of adipogenic differentiation (Fig. 3C), whereas there was a clear positive correlation between the fraction of CD106-positive cells at early passage and the amount of TG after adipogenic induction (Fig. 3D). These results indicated that the evaluation of CD106 at early passage is useful for predicting the differentiation potential of BMSCs.

Discussion

CD106/VCAM-1 is a cell surface glycoprotein, which binds to the $\alpha4\beta1$ and $\alpha4\beta7$ integrins [19]. A deficiency of CD106/VCAM-1 results in embryonic death with the absence of chorion-allantois fusion or multiple abnormalities in the heart in mice, but no significant abnormality was found in mesenchymal tissues during the embryonic stage [20]. CD106/VCAM-1 is associated with homing of HSCs, and CD106/VCAM-1-positive BMSCs, which may be MSCs, keep HSCs in their niche [21,22]. The binding to CD106/VCAM-1 activates integrin signaling, and cell migration or cytoskeletal organization is promoted [23]. But it is still unknown whether the integrin signaling influences the differentiation potential of BMSCs.

We have found that the fraction of CD106-positive cells in primary cultured-BMSC varied considerably among donors, although the same procedure was applied in all cases. The fraction of CD106 did not show any significant correlation with the sex or age of the donor (data not shown). Expression of CD106 is regulated by several cytokines [24], and some of them are produced by hematopoietic cells in bone marrow, which therefore may determine the number of CD106-positive cells at the beginning of the culture.

The negative correlation between CD106/VCAM-1 expression and the osteogenic property of ihBMSC seemed to contradict the idea of CD106/VCAM-1 as an MSC marker. We have no clear explanation for this phenomenon, but it should be considered that a considerable number of BMSCs have already committed to the osteogenic lineage before in vitro culture, among which some are ALP-positive but others may not be [25]. The expression of CD106/VCAM-1 was lost during the osteogenic differentiation (data not shown), suggesting the loss of CD106/VCAM-1 expression in osteogenic precursors. Therefore the osteogenic potential of each huBM strain evaluated in the current study may be determined by the number of osteogenic precursors negative for CD106/VCAM-1, but not of MSCs positive for CD106/VCAM-1, which would lead to the negative correlation observed in this study.

We also have found that the fraction of CD106-positive cells was positively correlated to the production of adipogenesis, which is compatible with the idea that CD106-positive cells include stem cells with adipogenic potential. As far as we know, there are no useful markers for predicting the adipogenic potential of BMSCs. Irrespective of the adipogenic potential, the amount of TG was below the detectable level (Fig. 3C), and no expression of the PPARγ

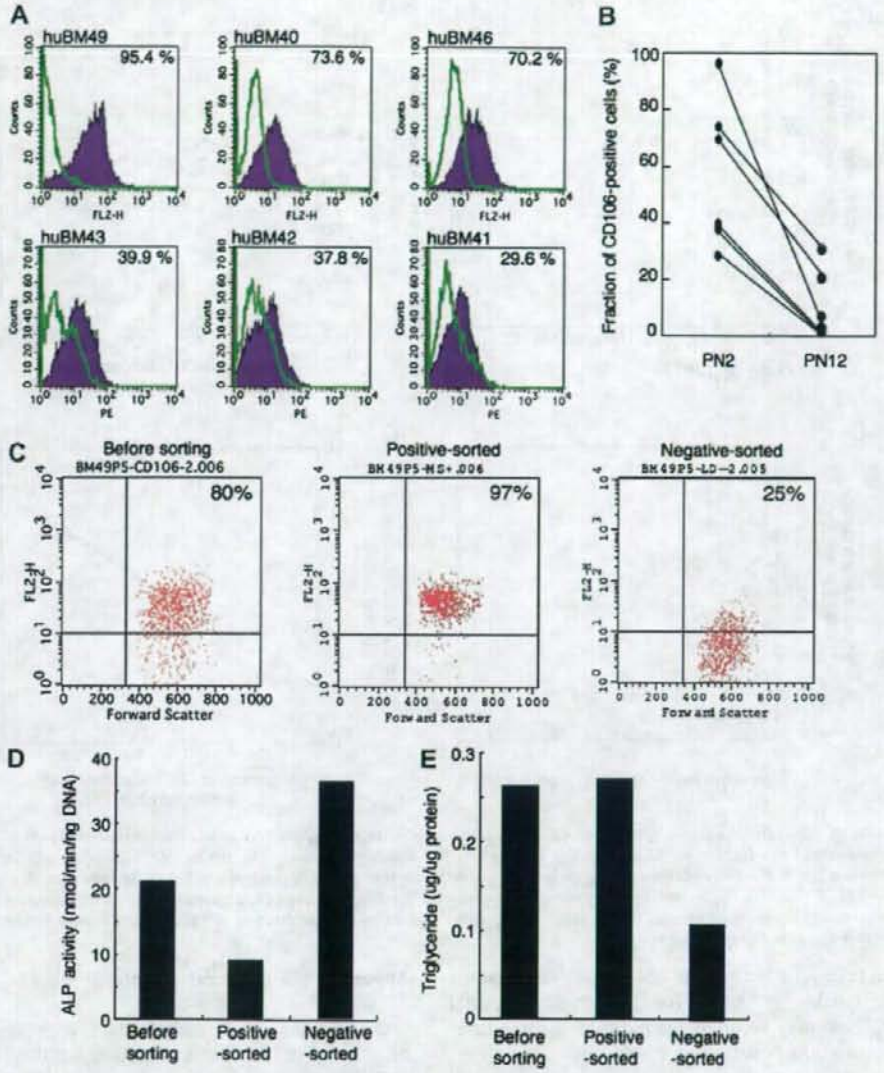

Fig. 2. The expression of CD106 correlated with the differentiation potential in primary BMSC. (A) Fraction of CD106-positive cells in six huBM strains. (B) Passage-dependent reduction of CD106-positive cells in primary BMSC. (C) Fraction of CD106 positive cells in huBM49 before and after the sorting by anti-CD106 Ab. (D) ALP activity after osteogenic induction in each cell population. (E) TG amounts after adipogenic induction in each cell population.

gene was observed (data not shown) in any BMSC strains before the adipogenic induction. Therefore, CD106 is the first cell surface marker to indicate the adipogenic potential of BMSC. Whether CD106/VCAM-1 is functionally involved in the promotion of adipogenesis is not known. That CD106/VCAM-1 knockout mice showed an apparently normal generation of mesenchymal tissue does not support a functional role for CD106/VCAM-1 in adipogenesis [20].

Whatever the mechanisms, the predictive power of CD106/VCAM-1 for osteogenic potential is quite valuable in the clinical application of BMSCs for bone regeneration. As far as we know, there are no useful markers for predicting the differentiation potential of BMSCs. The establishment of a standard method to evaluate osteogenic potential is one of the topics in bone regeneration therapy using MSCs, and a number of candidates have been proposed including ALP activity [26]. We have found,

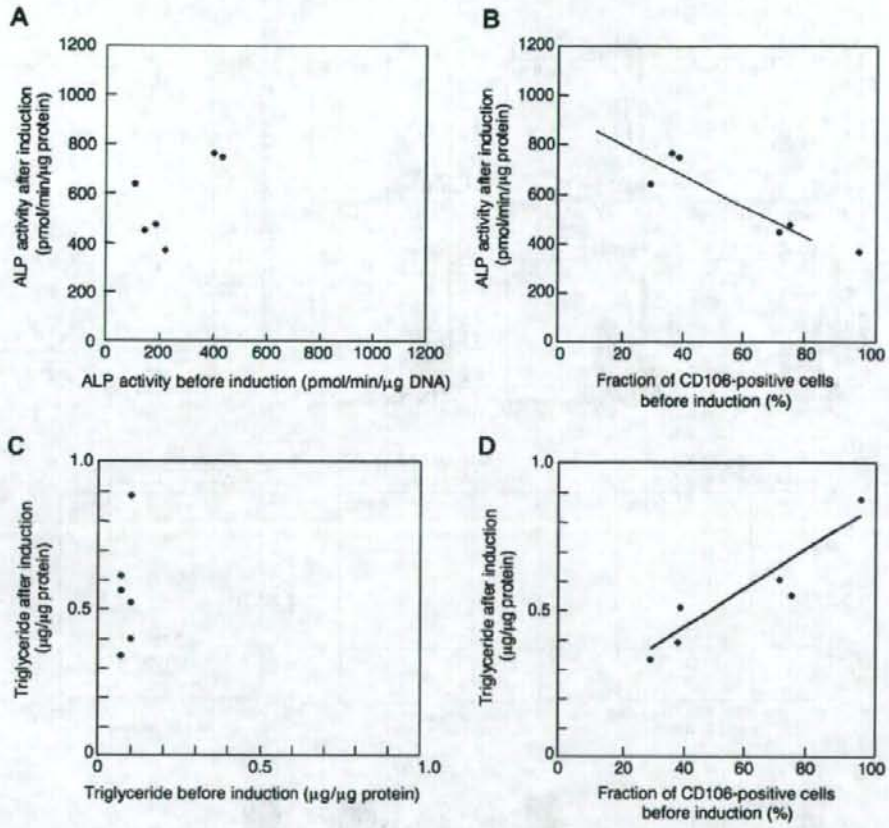

Fig. 3. Prediction of differentiation property based on CD106 expression in primary BMSCs. (A) Relationship between the ALP activity after the osteogenic induction and the fraction of CD106-positive cells before the induction in six huBM strains. No definite association was found. (B) Relationship between the ALP activity after the osteogenic induction and the fraction of CD106-positive cells before the induction. A negative association was found ($r = 0.86$, $P = 0.005$). (C) Relationship between the amount of TG before and after the adipogenic induction. No definite association was found. (D) Relationship between the amount of TG after the adipogenic induction and the fraction of CD106-positive cells before the induction. A positive association was found ($r = 0.91$, $P = 0.005$).

however, that the ALP activity of BMSCs at early passage was not a reliable indicator for osteogenic potential (Fig. 3A). CD106 may be a reliable indicator for the osteogenic differentiation potential of BMSC.

Acknowledgments

The authors thank Drs. Koichi Nishijo, and Tatsuya Ishibe for advice, and Drs. Takeshi Sakamoto and Hiromu Ito for clinical samples. This work was supported by the New Energy and Industrial Technology Development Organization (NEDO) with a project entitled Development of Evaluation Technology for Early Introduction of Regenerative Medicine, and also by Grants-in-aid for Scientific Research from the Japan Society for the Promotion of Science, from the Ministry of Education, Culture, Sports, Science, and Technology, and from the Ministry of Health, Labour, and Welfare.

Appendix A. Supplementary data

Supplementary data associated with this article can be found, in the online version, at doi:10.1016/j.bbrc.2007.10.149.

References

[1] M.F. Pittenger, A.M. Mackay, S.C. Beck, R.K. Jaiswal, R. Douglas, J.D. Mosca, M.A. Moorman, D.W. Simonetti, S. Craig, D.R. Marshak, Multilineage potential of adult human mesenchymal stem cells, Science 284 (1999) 143–147.

[2] E.M. Horwitz, P.L. Gordon, W.K.K. Koo, J.C. Marx, M.D. Neel, R.Y. McNall, L. Muul, T. Hofmann, Isolated allogenic bone marrow-derived mesenchymal cells engraft and stimulate growth in children with osteogenesis imperfecta: implications for cell therapy of bone, Proc. Natl. Acad. Sci. USA 13 (2002) 8932–8937.

[3] R. Kuroda, K. Ishida, T. Matsumoto, T. Akisue, H. Fujioka, K. Mizuno, H. Ohgushi, S. Wakitani, M. Kurosaka, Treatment of a full-thickness articular cartilage defect in the femoral condyle of an athlete

with autologous bone-marrow stromal cells, Osteoarthr. Cartilage 15 (2007) 226–231.
[4] S. Gronthos, P.J. Simmons, The growth factor requirements of STRO-1-positive human bone marrow stromal precursors under serum-deprived conditions in vitro, Blood 4 (1995) 929–940.
[5] H. Aslan, Y. Zilberman, L. Kandel, M. Liebergall, R.J. Oskouian, D. Gazit, Z. Gazit, Osteogenic differentiation of noncultured immunoisolated bone marrow-derived CD105^{+} cells, Stem Cells 24 (2006) 1728–1737.
[6] N. Quirici, D. Soligo, P. Bossolasco, F. Servida, C. Lumini, G.L. Deliliers, Isolation of bone marrow mesenchymal stem cells by anti-nerve growth factor receptor antibodies, Exp. Hematol. 30 (2002) 783–791.
[7] K. Mareschi, I. Ferrero, D. Rustichelli, S. Aschero, L. Gammaitoni, M. Aglietta, E. Madon, F. Fagioli, Expansion of mesenchymal stem cells isolated from pediatric and adult donor bone marrow, J. Cell. Biol. 97 (2006) 744–754.
[8] M. Honczarenko, Y. Le, M. Swierkowski, I. Ghiran, A.M. Glodek, L.E. Silberstein, Human bone marrow stromal cells express a distinct set of biologically functional chemokine receptors, Stem Cells 24 (2006) 1030–1041.
[9] S. Gronthos, A.C.W. Zannettiono, S.J. Hay, S. Shi, S.E. Graves, A. Kortesidis, P.J. Simmons, Molecular and cellular characterization of highly purified stromal stem cells derived from human bone marrow, J. Cell. Sci. 116 (2003) 1827–1835.
[10] T. Okamoto, T. Aoyama, T. Nakayama, T. Nakamata, T. Hosaka, K. Nishijo, T. Nakamura, T. Kiyono, J. Toguchida, Clonal heterogeneity in differentiation potential of immortalized human mesenchymal stem cells, Biochem. Biophys. Res. Commun. 295 (2002) 354–361.
[11] T. Mori, T. Kiyono, H. Imabayashi, Y. Takeda, K. Tsuchiya, S. Miyoshi, H. Makino, K. Matsumoto, H. Saito, S. Ogawa, M. Sakamoto, J. Hata, A. Umezawa, Combination of hTERT and bmi-1, E6, or E7 induces prolongation of the life span of bone marrow stromal cells from an elderly donor without affecting their neurogenic potential, Mol. Cell. Biol. 12 (2005) 5183–5195.
[12] B.M. Abdallah, M. Haack-Sorensen, J.S. Burns, B. Elsnab, F. Jakob, P. Hokland, M. Kassem, Maintenance of differentiation potential of human bone marrow mesenchymal stem cells immortalized by human telomerase reverse transcriptase gene in despite of extensive proliferation, Biochem. Biophys. Res. Commun. 326 (2005) 527–538.
[13] Y. Shima, T. Okamoto, T. Aoyama, K. Yasura, T. Ishibe, K. Nishijo, K.R. Shibata, Y. Kohno, K. Fukiage, S. Otsuka, D. Uejima, T. Nakayama, T. Nakamura, T. Kiyono, J. Toguchida, In vitro transformation of mesenchymal stem cells by oncogenic H-ras^{Val12}, Biochem. Biophys. Res. Commun. 353 (2007) 60–66.
[14] K.R. Shibata, T. Aoyama, Y. Shima, K. Fukiage, S. Otsuka, M. Furu, Y. Kohno, K. Ito, S. Fujibayashi, M. Neo, T. Nakayama, T. Nakamura, J. Toguchida, Expression of the p16INK4A gene is associated closely with senescence of human mesenchymal stem cells, and potentially silenced by DNA methylation during in vitro expansion, Stem Cells 9 (2007) 2371–2382.
[15] E.J. Caterson, L.J. Nesti, K.G. Danielson, R.S. Tuan, Human marrow-derived mesenchymal progenitor cells: isolation, culture expansion, and analysis of differentiation, Mol. Biotechnol. 20 (2002) 245–256.
[16] L.J. Foster, P.A. Zeemann, C. Li, M. Mann, O.N. Jensen, M. Kassem, Differential expression profiling of membrane proteins by quantitative proteomics in a human mesenchymal stem cell line undergoing osteoblast differentiation, Stem Cells 23 (2005) 1367–1377.
[17] R.J. Deans, A.B. Moseley, Mesenchymal stem cells: biology and potential clinical uses, Exp. Hematol. 28 (2000) 875–884.
[18] E.A. Jones, S.E. Kinsey, A. English, R.A. Jones, L. Straszynski, D.M. Meredith, A.F. Markham, A. Jack, P. Emery, D. McGonagle, Isolation and characterization of bone marrow multipotential mesenchymal progenitor cells, Arthritis Rheum. 12 (2002) 3349–3360.
[19] J.M. Bergelson, M.E. Hemler, Integrin-ligand binding. Do integrins use a 'MIDAS touch' to grasp an Asp?, Curr. Biol. 6 (1995) 615–617.
[20] L. Kwee, S. Baldwin, H.M. Shen, C.L. Stewart, C. Buck, C.A. Buck, M.A. Labow, Defective development of the embryonic and extraembryonic circulatory systems in vascular cell adhesion molecule (VCAM-1) deficient mice, Development 121 (1995) 489–503.
[21] I.B. Mazo, U.H. von Andrian, Adhesion and homing of blood-borne cells in bone marrow microvessels, J. Leukoc. Biol. 66 (1999) 25–32.
[22] T. Lapidot, I. Petit, Current understanding of stem cell mobilization: the roles of chemokines, proteolytic enzymes, adhesion molecules, cytokines, and stromal cells, Exp. Hematol. 30 (2002) 973–981.
[23] C. Kummer, M.H. Ginsberg, New approaches to blockade of alpha4-integrins, proven therapeutic targets in chronic inflammation, Biochem. Pharmacol. 72 (2006) 1460–1468.
[24] T. Collins, M.A. Read, A.S. Neish, M.Z. Whitley, D. Thanos, T. Maniatis, Transcriptional regulation of endothelial cell adhesion molecules: NF-κB and cytokine-inducible enhancers, FASEB J. 9 (1995) 899–909.
[25] M.W. Long, J.A. Robinson, E.A. Ashcraft, K.G. Mann, Regulation of human bone marrow-derived osteoprogenitor cells by osteogenic growth factors, J. Clin. Invest. 95 (1995) 881–887.
[26] H. Kotobuki, M. Hirose, H. Machida, Y. Katou, K. Muraki, Y. Takakura, H. Ohgushi, Viability and osteogenic potential of cryopreserved human bone marrow-derived mesenchymal cells, Tissue Eng. 11 (2005) 663–673.

Osteoarthritis and Cartilage (2009) 17, 529–538

doi:10.1016/j.joca.2008.09.003

Osteoarthritis and Cartilage

International Cartilage Repair Society

OARSI OSTEOARTHRITIS RESEARCH SOCIETY INTERNATIONAL

PGE2 signal *via* EP2 receptors evoked by a selective agonist enhances regeneration of injured articular cartilage

S. Otsuka M.D.†‡, T. Aoyama M.D., Ph.D.†*, M. Furu M.D.†§, K. Ito M.D.†‡, Y. Jin M.D.†, A. Nasu M.D.†§, K. Fukiage M.D.†§, Y. Kohno M.D., Ph.D.†§, T. Maruyama Ph.D.‖, T. Kanaji‖, A. Nishiura Ph.D.‖, H. Sugihara‖, S. Fujimura‖, T. Otsuka M.D., Ph.D.‡, T. Nakamura M.D., Ph.D.§ and J. Toguchida M.D., Ph.D.†

† *Department of Tissue Regeneration, Institute for Frontier Medical Sciences, Kyoto University, Kyoto, Japan*

‡ *Department of Orthopaedic Surgery, Graduate School of Medical Sciences, Nagoya City University, Nagoya, Japan*

§ *Department of Orthopaedic Surgery, Graduate School of Medicine, Kyoto University, Kyoto, Japan*

‖ *Ono Pharmaceutical Co. Ltd., Osaka, Japan*

Summary

Objective: The effect of the prostaglandin E2 (PGE2) signal through prostaglandin E receptor 2 (EP2) receptors on the repair of injured articular cartilage was investigated using a selective agonist for EP2.

Methods: Chondral and osteochondral defects were prepared on the rabbit femoral concave in both knee joints, and gelatin containing poly-lactic-co-glycolic acid microspheres conjugated with or without the EP2 agonist was placed nearby. Animals were sacrificed at 4 or 12 weeks post-operation, and regenerated cartilage tissues and subchondral structure remodeling were evaluated by histological scoring. The quality of regenerated tissues was also evaluated by the immunohistochemical staining of EP2, type II collagen, and proliferating cell nuclear antigen (PCNA). As an evaluation of side effects, the inflammatory reaction of the synovial membrane was analyzed based on histology and the mRNA expression of matrix metalloproteinase3 (MMP3), tissue inhibitor of metalloproteinase 3 (TIMP3), and interleukin-1β (IL-1β). Also, the activity of MMP3 and the amount of tumor necrosis factor-α (TNF-α) and C-reactive protein in joint fluid were measured.

Results: In both models, the EP2 agonist enhanced the regeneration of the type II collagen-positive tissues containing EP2- and PCNA-positive chondrocytes, and the histological scale of regenerated tissue and subchondral bone was better than that of on the control side, particularly at 12 weeks post-operation. No inflammatory reaction in the synovial membrane was observed, and no induction of pro-inflammatory cytokines was found in joint fluid.

Conclusion: Selective stimulation of the PGE2 signal through EP2 receptors by a specific agonist promoted regeneration of cartilage tissues with a physiological osteochondral boundary, suggesting the potential usefulness of this small molecule for the treatment of injured articular cartilages.

Key words: PGE2, EP2, Agonist, Cartilage, Defect, Repair, Therapeutic drug, Osteoarthritis.

Introduction

Chondrocytes in articular cartilage are differentiated cells with minimum proliferating potential and low metabolic activity[1]. Because these cells are fully responsible for the production of cartilage matrix consisting of collagens and proteoglycans, considerable damage to articular cartilage is unrepairable, initiating a sequence of catabolic events leading to a pathological condition known as osteoarthritis (OA). Although inflammation of the synovium and the destruction of subchondral bone integrity also play an important role in the progression of OA, the poor regenerative capacity of chondrocytes is the major disease-causing factor[1,2]. In the early stages of OA, however, not only catabolic but also anabolic activity is enhanced in chondrocytes. As catabolic activity, chondrocytes produce several catabolic cytokines such as interleukin-1 (IL-1), which in turn induce the production of proteinases such as matrix metalloproteinases (MMPs) and a disintegrin-like and metalloprotease with thrombospondin (ADAMTS) leading to the destruction of the matrix network[2]. As anabolic activity, chondrocytes produce anabolic cytokines such as the bone morphogenic protein (BMP) family and insulin like growth factor-1 (IGF-1), which induce the synthesis of collagens and initiate the proliferation of chondrocytes themselves making osteophytes at the periphery[2]. A disruption of the equilibrium between the catabolic and anabolic activities results in catastrophic damage to articular cartilage. In adult articular cartilage, the equilibrium leans toward catabolic activity; the proliferation of chondrocytes is decreased and the subchondral structure is weak.

The role of prostaglandin E2 (PGE2) in the development of OA is controversial. Pro-inflammatory signal mediators such as IL-1 and tumor necrosis factor-α (TNF-α) induce

*Address correspondence and reprint requests to: Dr T. Aoyama, M.D., Ph.D., Department of Tissue Regeneration, Institute for Frontier Medical Sciences, Kyoto University, 53 Kawahara-cho, Shogoin, Sakyo-ku, Kyoto 606-8507, Japan. Tel: 81-75-751-4107; Fax: 81-75-751-4646; E-mail: blue@frontier.kyoto-u.ac.jp

Received 13 April 2008; revision accepted 2 September 2008.

the synthesis of PGE2 by promoting the expression or activities of cyclooxygenase (COX)-2 and microsomal PGE synthase-1[3]. The synthesized PGE2 promotes IL-1 expression as a positive feedback mechanism, degrades the cartilage matrix[4], and finally induces apoptosis of chondrocytes[5], indicating a catabolic role for PGE2 in OA. In some reports, however, anabolic effects of PGE2 were demonstrated[1,3]. PGE2 opposed the effect of IL-1 by down-regulating type I collagen[6] and stimulating type II collagen gene expression[7,8]. Also, PGE2 stimulated the synthesis of proteoglycan and collagen through the induction of IGF-1-binding protein[9], and induced the proliferation of rat chondrocytes as demonstrated by an increase in the incorporation of [^{3}H]-thymidine[9].

Several factors are involved in these controversial findings including experimental design, the level of PGE2 expression, the balance with other pro-inflammatory cytokines, and most notably, the variety of receptors. PGE2 exerts its biological effect through one of four receptors, EP1, EP2, EP3, or EP4. The development of specific agonists and antagonist for each receptor enables the understanding of the receptor-specific signal transduction mechanism and its consequence. Signals through EP1 and EP3 coupled by G_i protein increase the intra-cellular Ca^{2+} concentration, and those through EP2 and EP4 coupled by G_s protein increase cyclic adenosine monophosphate (cAMP). Although the second messenger is common, the amide acid identity is only 31% between EP2 and EP4. EP4 (513 amino acids) has the longest intra-cellular C terminal, but EP2 (362 amino acids) has a compact structure. In osteoclastogenesis, the EP2 and EP4 mediate the induction of receptor activator of nuclear factor-kappa B (NF-κB) ligand (RANKL), but the extent of the contribution by each receptor is different. Although both EP2 and EP4 are expressed in dendritic cell, EP4 has selective action for cell migration. This selectivity of EP4 may be caused by the fact that EP4 but not EP2 couples to phosophatidylinositol 3-kinase in addition to cAMP[10].

We have previously demonstrated that EP2 was the major PGE2 receptor in articular chondrocytes[11]. And a specific agonist for EP2 not EP4 promoted the growth of mouse and human chondrocytes by up-regulating the expression of growth-promoting genes such as the *cyclin D* gene stimulating the increase of cAMP[11]. The protein structure and function of EP2 are conserved between many species, and the amino acid homology between the human and mouse, rat, or rabbit is 88.2, 84.9, and 90.2%, respectively. The effect of the EP2 agonist on chondrocytes was confirmed in a rat organ culture system, suggesting the possible application of this small molecule as a new therapeutic tool for injured articular cartilage[11].

In this study, we investigated the effect of an EP2 agonist on injured articular cartilage *in vivo* using rabbit knee joints and also on other joint structures such as the synovium and subchondral bone.

Materials and methods

REAGENTS

Microspheres loaded with the selective EP2 agonist, ONO-8815Ly[12] prepared by the emulsion–solvent evaporation method as described[13]. Briefly, ONO-8815Ly was dissolved in purified water as the inner water phase and polylactic-co-glycolic acid (PLGA) was dissolved in dichloromethane as the oil phase. The water/oil (w/o) emulsion was gradually added to the outer water phase containing polyvinyl alcohol (PVA, 0.1%, w/v), NaCl (2%, w/v) and maltose (2%, w/v) adjusted to pH 3.0, under stirring with a turbine-shaped mixer at 5000 rpm to obtain a water/oil/water emulsion. Then PLGA microspheres were formed in the outer water phase after the evaporation of dichloromethane. In order to recover the microspheres without a free form of ONO-8815Ly, the suspension was centrifuged at 3000 rpm for 10 min and the microspheres were precipitated. The washed microsphere precipital was lyophilized to remove residual organic solvent and water, and then dried solid ONO-8815Ly-loaded microspheres were recovered. ONO-8815Ly-loaded microspheres were dispersed in purified water, and then gelatin aqueous solution (20%, w/w) was poured into the microsphere suspension. The resultant microsphere–gelatin suspension was poured into a polypropylene container and placed in a refrigerator for 12 h to form a gel. Afterward, glutaraldehyde aqueous solution (12.5 μg/ml) was poured into the microsphere–gelatin gel and placed in the refrigerator for 24 h for the crosslink reaction. The gel sheet obtained was placed into glycine aqueous solution. These procedures were performed repeatedly. Small cylinder-shaped gelatin hydrogels containing either 80 or 400 μg of ONO-8815 were obtained by hollowing out the gelatin hydrogel sheet.

SURGICAL PROCEDURE

The institutional animal research committee, according to the guidelines for Animal Experiments of Kyoto University, approved this investigation. Japanese white rabbits (Shimizu Laboratory Supplies Co., Kyoto, Japan) were at least 5 months old and had a body weight of 3 kg.

Two types of cartilage defect on the femoral concave of the patello-femoral joint were made according to depth (Supplementary Fig. 1). A chondral defect, which involved the osteochondral boundary (tide mark) but not subchondral bone, was made using a punch without damaging the subchondral bone (5.0 mm in diameter) [Supplementary Fig. 1(A–C)]. An osteochondral defect was made using a hand drill [4.0 mm in diameter and 5.0 mm in depth, Supplementary Fig. 1(D–F)]. By preliminary experiments, we have confirmed that both types of defects were not healed spontaneously (data not shown).

The same type of defect was created in both femurs, and a cylinder-shaped gelatin hydrogel containing PLGA microspheres conjugated with ONO-8815 (80 or 400 μg) was placed into the infra-patellar fat pad on one side (thereafter designated EP2 agonist-treated samples), and gelatin hydrogels without microspheres were placed on the contralateral side (contralateral samples). The animals were allowed to move. To exclude any possible effect of ONO-8815 in the systemic circulation, controls were established, in which empty gelatin hydrogel was placed in bilateral knee joints after creating each defect model (control samples, $N = 3$). Animals were sacrificed and evaluated at 4 ($N = 5$) and 12 ($N = 8$) weeks after the operation.

HISTOLOGICAL EVALUATION

Cartilage samples were fixed overnight at 4°C in a 10% formalin solution, decalcified by formic acid, and embedded in paraffin. Then sections were cut at 6 mm through the center of each defect, stained with Safranin-O/Fast Green and hematoxylin–eosin (HE), examined in a blinded manner by two evaluators, and graded with the use of a modified Wakitani histological scale[14]. The reconstitution of articular chondrocytes and subchondral bone connections (category II on the modified Wakitani scale) was partially evaluated by grading from 0 to 7. Specimens of the synovium around the infra-patellar fat pads were fixed in 10% formalin, embedded in paraffin, and cut into 6 μm thick sections for histological evaluation. Sections were stained with HE and the severity of synovial lesions was graded according to the histological scoring system, based on the hyperplasia of synovial lining cells, hypertrophy of the synovial lining layer, infiltration of inflammatory cells, proliferation of granulation tissue, and vascularization[15]. Two independent observers blinded to the treatment groups graded all sections.

IMMUNOHISTOCHEMISTRY

Immunostaining of proliferating cell nuclear antigen (PCNA; diluted 1:100; Dako, Glostrup, Denmark) and alpha1 type II collagen (diluted 1:50; Daiichi Fine Chemical, Toyama, Japan) was performed as previously mentioned[11]. Immunostaining of EP2 (diluted 1:100; Cayman Chemical Co., Ann Arbor, MI) was performed as described by Fukuda *et al.*[16]. Under the microscope (400×), all cells and PCNA-positive cells were counted by two individuals. Three visual fields were randomly selected by each observer, and, therefore, each specimen was evaluated three times. Then labeling index was calculated as the mean of these three values. The relative increase in PCNA-positive cells was expressed as the ratio of the labeling index of the EP2 agonist-treated sample vs that of the contralateral sample. The labeling index of control sample was also calculated as a value relative to those of contralateral sample.

ASSAY OF MMP3, TNF-α, AND C-REACTIVE PROTEIN (CRP) IN SYNOVIAL FLUID

After the injection of 1 ml of saline solution into the knee joint, synovial fluid was obtained by arthrocentesis through a sub-patellar approach. Synovial fluid was aspirated as far as possible from the knee joint. After

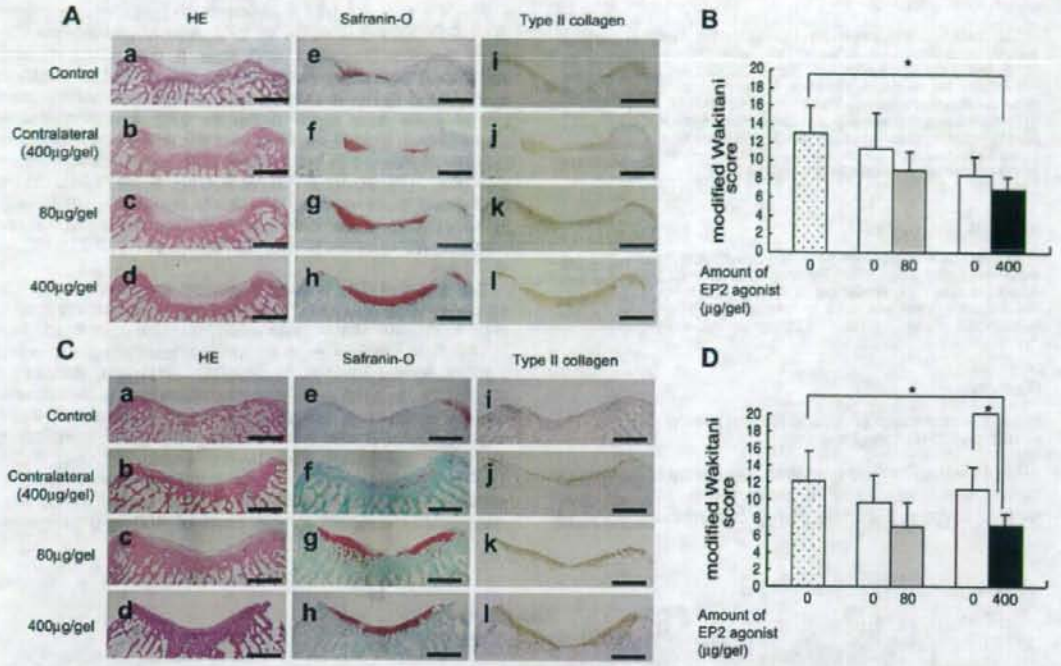

Fig. 1. Effects of EP2 agonist on the regeneration of chondral defects. Histological evaluations were performed at 4 (A) or 12 (C) weeks after the operation. Each specimen was prepared from control samples (a, e, and i), contralateral (b, f, and j), or EP2 agonist-treated (c, g, and k, 80 μg/gel; d, h and l; 400 μg/gel) samples. The quality of regenerated tissues was analyzed by HE staining (a–d), Safranin-O staining (e–h), or immunohistochemical staining with anti-type II collagen Ab (i–l). Magnification 2×. Bar = 2.0 mm. The quality of regenerated tissues was also evaluated with a modified Wakitani histological scale at 4 (B) and 12 (D) weeks after the operation. Dotted and open boxes indicate the scale for control and contralateral samples, respectively, $^{*}P < 0.05$.

the specimen was centrifuged at 1500 rpm for 20 min, the supernatant was drawn out and stored at −70°C[17]. MMP3 activity was measured with a MMP3 fluorimetric drug discovery kit (BIOMOL International LP, Plymouth Meeting, PA). TNF-α levels in joint fluids were measured using a sandwich enzyme-linked immunosorbent assay (ELISA) with specific anti-TNF-α polyclonal antibodies (Abs) (BD Pharmingen, San Diego, CA). Briefly, microtiter plates were coated with 50 μl of anti-rabbit. TNF-α capture Abs (4 mg/ml) overnight at 4°C, then washed twice with phosphate buffered saline (PBS) containing 0.05% Tween 20 and blocked overnight at 4°C with 10% fetal bovine serum (FBS) in PBS. After the plates were washed four times, standards and samples (100 μl) were incubated in duplicate overnight at 4°C. Plates were again washed and a biotin-conjugated anti-TNF-α secondary Ab (2 mg/ml) was added for 1 h at room temperature. A 30-min incubation with a 1:400 dilution of avidin–peroxidase (Sigma) followed extensive washing of the plate. Finally, TMBlue (Intergen, Milford, MA) substrate was added (100 μl/well) and incubated at room temperature for 30 min. The absorbance was read at 450 nm with an UVmax microplate reader (Molecular Devices, Menlo Park, CA). Rabbit CRP was measured with a rabbit CRP ELISA kit (Alpha Diagnostic International Inc., San Antonio, TX).

REVERSE TRANSCRIPTION-POLYMERASE CHAIN REACTION (RT-PCR)

Total RNA was extracted from frozen synovial samples using TRIzol reagent (Invitrogen, Carlsbad, CA) and 1 μg was reverse transcribed for single-stranded cDNA using the oligo (dT) primer and Superscript II reverse transcriptase (Invitrogen). RT-PCR was performed in duplicate for each sample using primers listed in Table I[18,19].

Table I
Primers used in the RT-PCR analyses

Gene	Primers*	Size (bp)	Position	Accession no.
MMP3	CTGGAGGTTTGATGAGAAGA CAGTTCATGCTCGAGATTCC	336	1278–1297 1597–1616	NM_001082280
TIMP1	GCAACTCCGACCTTGTCATC AGCGTAGGTCTTGGTGAAGC	326	122–141 428–447	NM_001082232
IL-1β	TGCTGTCCAGACGAGGGCAT ACTCTCCAGCTGCAGGGTAG	473	210–229 664–683	NM_001082201
GAPDH	GTCAAGGCTGAGAACGGGAA GCTTCACCACCTTCTTGATG	613	246–265 839–858	NM_001082253

*All primer sequences are written from 5′ to 3′. The top sequence is the sense primer and the bottom sequence is the anti-sense primer.

QUANTITATIVE RT-PCR

The levels of mRNA expression of genes (*MMP3, TIMP1, IL-1β* and *glyceraldehyde 3-phosphate dehydrogenase* (*GAPDH*)) were quantified by SYBR Green (Applied Biosystems, Foster City, CA) real time PCR with the ABI PRISM 377 Sequence Detection System (Applied Biosystems). Each gene amplification efficiency was similar with *GAPDH*. All reactions were run in triplicate, and the mean value was used to calculate the ratio of target gene/*GAPDH* expression in each sample. Using the ratio in untreated sample as a standard (1.0), the relative ratio of the treated sample was presented as the relative expression level of the target gene[11].

STATISTICAL ANALYSES

All statistical analyses were performed using Statcel software. The results are shown as the mean ± SD. The analysis of variance (ANOVA) test was used to compare the differences in the scales between multiple groups. The Student's *T* test was used to compare the differences in the scales between two groups. A P value < 0.05 was considered significant.

Results

EP2 AGONIST PROMOTED TISSUE REGENERATION IN THE CHONDRAL DEFECT MODEL

Four weeks after the operation, the quality of regenerated tissues was analyzed by HE staining [Fig. 1(A, a–d)], Safranin-O staining [Fig. 1(A, e–h)], or immunohistochemical staining with anti-type II collagen Ab [Fig. 1(A, i–l)]. Most of regenerated tissues in EP2 agonist-treated samples were Safranin-O-positive and type II collagen-positive, suggesting the quality as hyaline cartilage. The quality of regenerated tissue evaluated by modified Wakitani histological scale was much better in EP2 agonist-treated samples than control samples, and the difference was statistically significant in the case of 400 μg/gel-treated samples [Fig. 1(B): 80 μg, $P = 0.08$; 400 μg, $P = 0.04$]. On the other hand, there were no statistically significant difference in histological scale between EP2 agonist-treated and contralateral samples [Fig. 1(B): 80 μg, $P = 0.21$; 400 μg, $P = 0.24$].

The effect of EP2 agonist treatment was much clear at 12 weeks after operation. In control and contralateral samples, the amount of regenerated tissues was much less than that found at 4 weeks after operation, and most of them were negative for Safranin-O or type II collagen [Fig. 1(C)]. In EP2 agonist-treated samples, regenerated tissues reached a considerable width, most of which were Safranin-O and type II collagen-positive indicating properties compatible with hyaline cartilage [Fig. 1(C)]. The histological scale of EP2 agonist-treated samples showed significantly better than that of control and also contralateral samples in the case of 400 μg/gel-treated

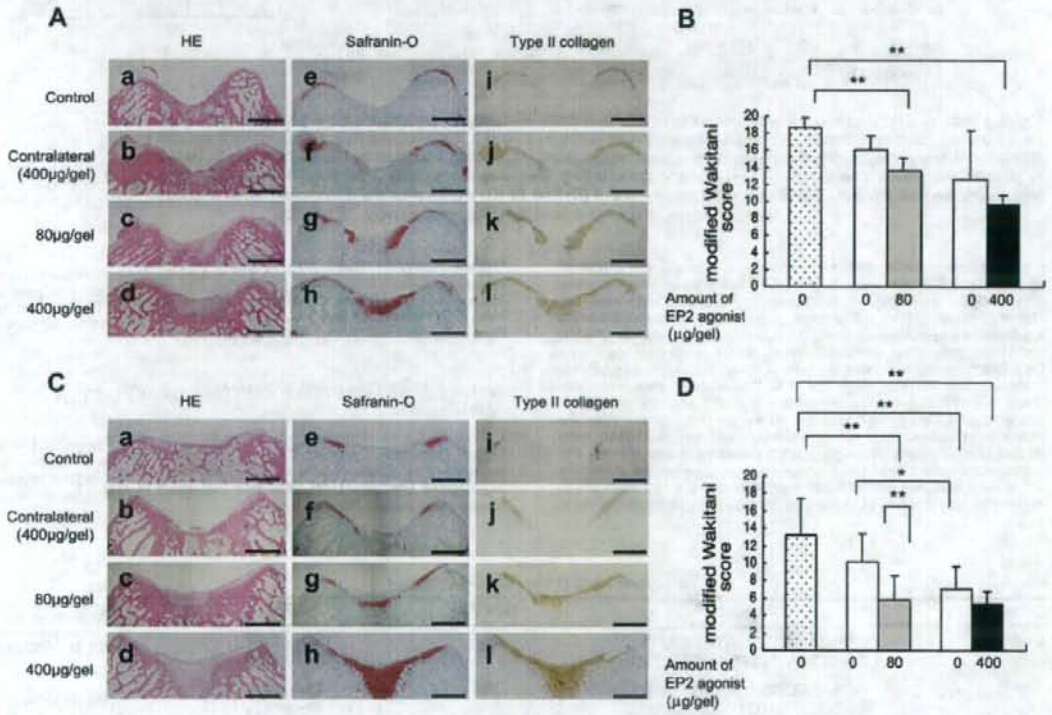

Fig. 2. Effects of EP2 agonist on the regeneration of osteochondral defects. Histological evaluations were performed at 4 (A) or 12 (C) weeks after the operation. Each specimen was prepared from control samples (a, e, and i), contralateral (b, f, and j), or EP2 agonist-treated (c, g, and k, 80 μg/gel; d, h and l; 400 μg/gel) samples. The quality of regenerated tissues was analyzed by HE staining (a–d), Safranin-O staining (e–h), or immunohistochemical staining with anti-type II collagen Ab (i–l). Magnification 2×. Bar = 2.0 mm. The quality of regenerated tissues was also evaluated with a modified Wakitani histological scale at 4 (B) and 12 (D) weeks after the operation. Dotted and open boxes indicate the scale for control and contralateral samples, respectively, $^{**}P < 0.01$; $^{*}P < 0.05$.

samples [Fig. 1(D): vs control, $P=0.02$; vs contralateral, $P=0.01$]. The histological scale of contralateral samples tended to be better than that of control samples, although there was no statistical significance [Fig. 1(C): 80 μg, $P=0.31$; 400 μg; $P=0.1$, Fig. 1(D): 80 μg, $P=0.2$; 400 μg; $P=0.35$].

EP2 AGONIST PROMOTED TISSUE REGENERATION IN THE OSTEOCHONDRAL DEFECT MODEL

To analyze the effect of the EP2 agonist on tissue regeneration in osteochondral lesions, an osteochondral defect model was created [Supplementary Fig. 1(C–E)]. At 4 weeks

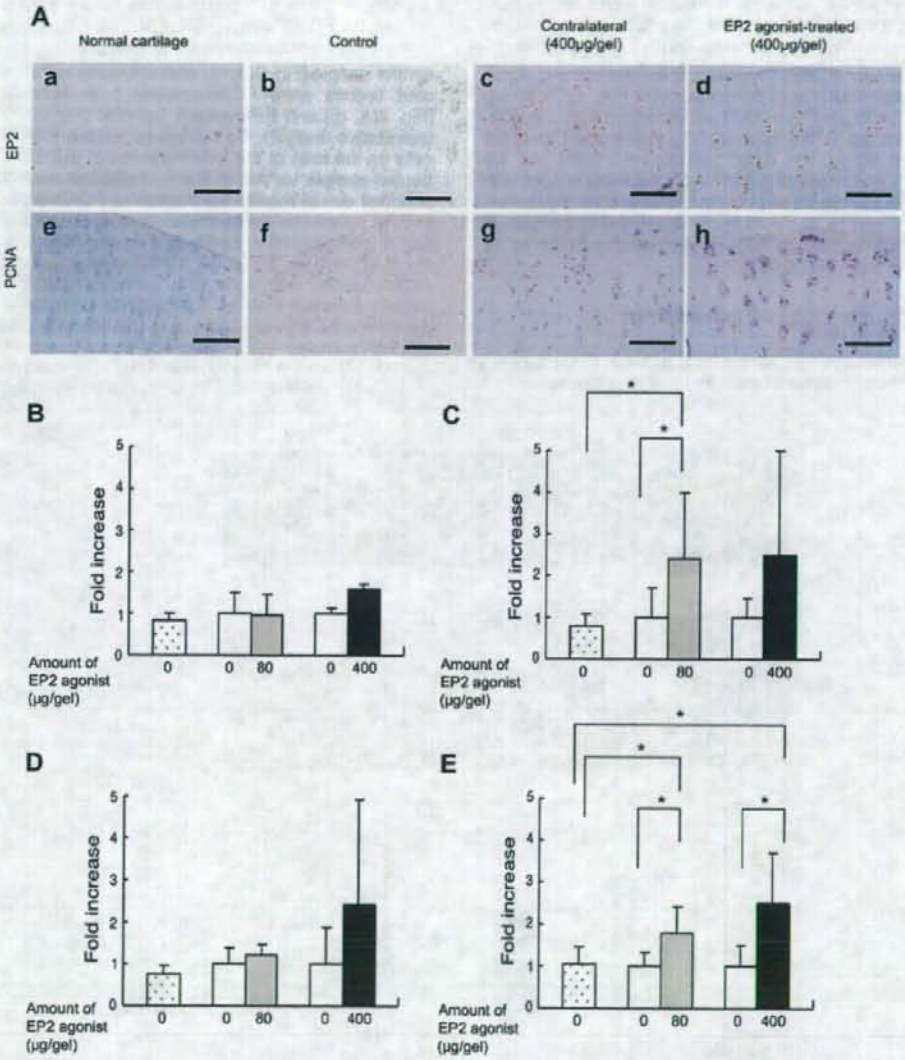

Fig. 3. EP2 agonist promotes proliferation of EP2-positive cells. A: Expression of EP2 and PCNA in normal and regenerated cartilage of chondral defect model. Specimens were prepared from a normal femur without any treatment (a and e), a control sample (b and f), a contralateral sample (c and g), and an EP2 agonist-treated (400 μg/gel) sample (d and h) at 12 weeks after the operation. Immunohistochemical staining was performed with anti-EP2 Ab (a–d) or anti-PCNA Ab (e–h). Bar = 100 μm. B–E: Quantitative analysis of PCNA-positive cells. Cells positive for PCNA staining were counted under the microscope, and a labeling index was calculated for each sample. The relative increase in PCNA-positive cells is expressed as the ratio of the labeling index of the EP2 agonist-treated sample (shaded bars) vs that of the contralateral sample (open bars). The labeling index of control sample relative to those of contralateral sample was indicated in dotted boxes. Samples were prepared from the chondral defect model at 4 weeks (B), chondral defect model at 12 weeks (C), osteochondral defect model at 4 weeks (D), and osteochondral defect model for 12 weeks (E), $^*P<0.05$.

after the operation, the osteochondral defects were filled with regenerated tissue in all cases, but there was a significant difference in histological scale between EP2 agonist-treated and control samples [Fig. 2(D): 80 μg, $P = 0.005$; 400 μg, $P = 0.0003$]. As in the chondral defect model, the difference was not significant between EP2 agonist-treated than contralateral samples [Fig. 2(D): 80 μg, $P = 0.07$; 400 μg, $P = 0.21$].

At 12 weeks after operation, the effect of EP2 agonist treatment was much evident. The osteochondral defect of EP2 agonist-treated samples was filled with Safranin-O and type II collagen-positive tissues [Fig. 2(C)], and the grading scale of EP2 agonist-treated samples showed and significantly better than that of control samples [Fig. 2(D): 80 μg, $P = 0.002$; 400 μg, $P = 0.0003$] and also than that of contralateral samples in the case of 80 μg/gel-treated samples [Fig. 2(D): 80 μg, $P = 0.006$; 400 μg, $P = 0.05$]. As we observed in the chondral defect model, the scale of contralateral samples tended to be better than that of control samples, and the difference was statistically significant in the case of contralateral sample in 400 μg/gel-treated animals at 12 weeks [Fig. 2(D), $P = 0.005$].

EP2 AGONIST STIMULATED THE PROLIFERATION OF EP2-POSITIVE CELLS

In normal cartilage, almost all cells were EP2-positive as we previously demonstrated in mice and human articular cartilage[11] [Fig. 3(A, a)]. Almost all cells in regenerated tissues of chondral defect model at 12 weeks after operation expressed the EP2 receptor in control [Fig. 3(A, b)], contralateral [Fig. 3(A, c)] and EP2-treated samples (400 μg/gel) [Fig. 3(A, d)]. Identical results were observed in samples harvested at 12 weeks after operation (data not shown), suggesting that the cartilage regeneration was conducted mainly by EP2-positive cells. To evaluate the proliferating ability of these EP2-positive cells, same specimens were used for PCNA staining [Fig. 3(A, e–h)]. Almost no cells were PCNA-positive in normal cartilage [Fig. 3(A, e)] and control sample [Fig. 3(A, f)], whereas some cells in regenerated tissues were PCNA-positive both in contralateral [Fig. 3(A, g)] and EP2-treated samples [Fig. 3(A, h)]. For quantitative analysis, we compared relative PCNA-positive cells as the ratio of the labeling index of the EP2 agonist-treated sample vs that of the contralateral sample. In the chondral defect model, the fraction of PCNA-positive cells in EP2 agonist-treated samples was almost the same as that in contralateral samples at 4 weeks [Fig. 3(B): 80 μg, $P = 0.47$; 400 μg, $P = 0.19$]. At 12 weeks, the fraction of PCNA-positive cells seemed to be higher in EP2 agonist-treated samples than in contralateral samples, although the difference was not convincing due to the wide variation among samples [Fig. 3(C): 80 μg, $P = 0.04$; 400 μg, $P = 0.12$]. In the osteochondral defect model, the fraction of PCNA-positive cells in EP2-treated samples was not

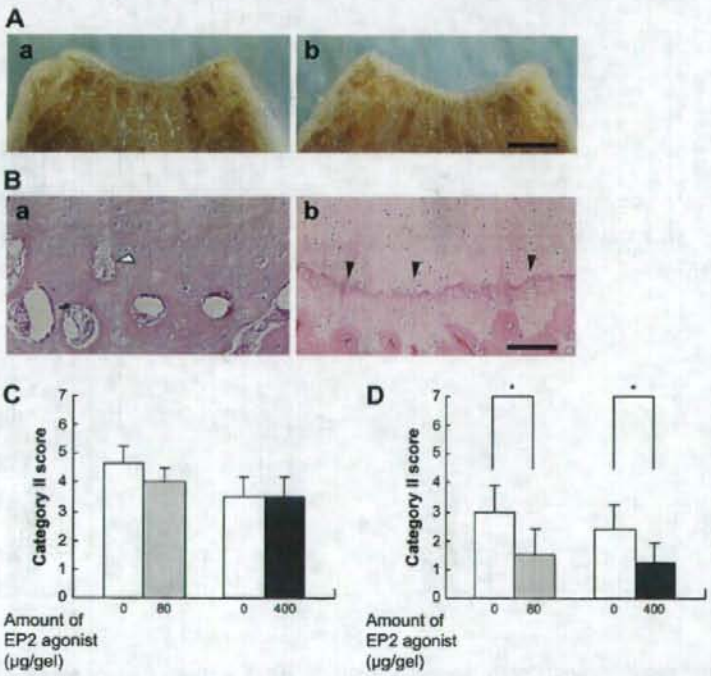

Fig. 4. Effect of EP2 agonist on remodeling of the deep layer zone in chondral defect model. A: Macroscopic view of specimens from contralateral sample (a) and EP2 agonist-treated (400 μg/gel) sample (b) of chondral defect model at 12 weeks after the operation. Bar = 4.0 mm. B: Microscopic view of the osteochondral boundary in the specimens presented in (A). (a) Contralateral sample, (b) EP2 agonist-treated (400 μg/gel) sample. Note that there was no clear boundary, and vascular invasion into articular chondrocytes (white arrowhead) was observed in (a), whereas a clear tidemark (black arrowhead) was formed in (b). Magnification 40×. Bar = 100 μm. C and D: Quantitative evaluation of the osteochondral boundary. The boundary formed between articular cartilage and subchondral bone was evaluated by category II scale of the modified Wakitani scale (0–7, 7 is worse). Samples were prepared from the chondral defect model at 4 weeks (C) and at 12 weeks (D), $^*P < 0.05$.

different from those in contralateral samples at 4 weeks [Fig. 3(D): 80 μg, $P=0.31$; 400 μg, $P=0.46$], but significantly higher at 12 weeks [Fig. 3(E): 80 μg, $P=0.02$; 400 μg, $P=0.02$]. In all settings, the labeling index of control samples showed no difference from those of contralateral samples [Fig. 3(B): $P=0.47$; Fig. 3(C): $P=0.31$; Fig. 3(D): $P=0.1$; Fig. 3(E): $P=0.43$].

EP2 AGONIST REPAIRED THE OSTEOCHONDRAL BOUNDARY

Reconstruction of the physiological boundary between articular cartilage and underlying bone tissue is important to maintain the mechanical and biological properties of articular cartilage. Macroscopical examination of EP2 agonist-treated (400 μg/gel) samples in chondral defect model at 12 weeks after operation showed a clear boundary between articular cartilage and subchondral bone [Fig. 4(A, b)]. Microscopical examination demonstrated the reconstruction of the tidemark [Fig. 4(B, b)]. These findings were not observed in contralateral samples. The boundary was not clear in macroscopical examination [Fig. 4(A, a)], and microscopical examination also showed no boundary with some vascular structures in the cartilaginous portion [Fig. 4(B, a)]. The difference was quantitatively evaluated using the category II scale of the modified Wakitani scale. There was no significant difference between EP2 agonist-treated and contralateral samples at 4 weeks [Fig. 4(C)], but the scale was significantly lower in the former than the latter at 12 weeks after operation [Fig. 4(D): 80 μg, $P=0.03$; 400 μg, $P=0.04$].

Similar findings were obtained in the osteochondral defect model (Fig. 5). EP2 agonist-treated (400 μg/gel) samples in osteochondral defect model at 12 weeks after operation the showed a clear boundary between articular cartilage and subchondral bone by macroscopical and microscopical examinations [Fig. 5(A, b and B, b)], which were not observed in contralateral samples [Fig. 5(A, a and B, a)]. Quantitative evaluation demonstrated that the boundary was much better formed in 400 μg/gel-, but not 80 μg/gel-treated samples than in contralateral samples at 12 weeks after operation [Fig. 5(D): 80 μg, $P=0.07$; 400 μg, $P=0.009$]. This difference was not observed in samples at 4 weeks [Fig. 5(C)]. These results suggest that the EP2 agonist improved the environment surrounding cartilage.

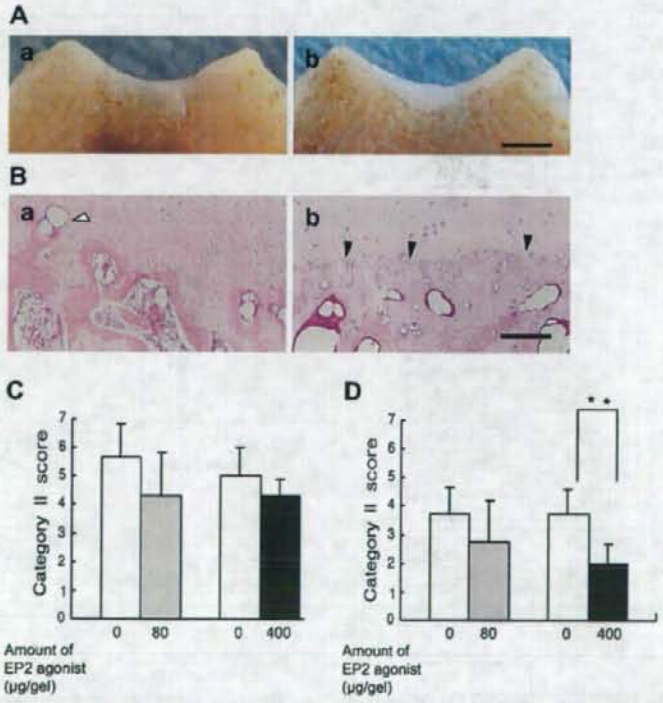

Fig. 5. Effect of EP2 agonist on remodeling of the deep layer zone in osteochondral defect model. A: Macroscopic view of specimens from contralateral sample (a) and EP2 agonist-treated (400 μg/gel) sample (b) of osteochondral defect model at 12 weeks after the operation. Bar = 4.0 mm. B: Microscopic view of the osteochondral boundary in the specimens presented in (A). (a) Contralateral sample (b) EP2 agonist (400 μg/gel)-treated sample. Note that there was no clear boundary, and vascular invasion into articular chondrocytes (white arrowhead) was observed in (a), whereas a clear tidemark (black arrowhead) was formed in (b). Magnification 40×. Bar = 100 μm. C and D: Quantitative evaluation of the osteochondral boundary. The boundary formed between articular cartilage and subchondral bone was evaluated by category II scale of the modified Wakitani scale (0–7, 7 is worse). Samples were prepared from the chondral defect model at 4 weeks (C) and at 12 weeks (D), $^{**}P<0.01$.

EP2 AGONIST DID NOT INDUCE INFLAMMATION OF THE SYNOVIUM

It is important whether the EP2 agonist induced unfavorable inflammation during the regeneration process. We evaluated the synovium based on mRNA expression and histological scoring, and also measured the amounts of cytokines in joint fluid at 4 weeks. PGE2 was reported to up-regulate the expression of the *MMP3*, *TIMP3*, and *IL-1β* genes[3]. The expression of these inflammation-related genes was analyzed by semi-quantitative [Fig. 6(A)] and quantitative RT-PCR [Fig. 6(B)] using samples taken at 4 weeks. No significant up-regulation was found in either gene even in samples treated with a larger amount of EP2 agonist [Fig. 6(B)]. The activity of MMP3 in joint fluid had almost the same value as found in untreated joints [Fig. 6(C)]. The amount of TNF-α or CRP in treated knee joints showed no significant change compared with that in normal joints either [Fig. 6(D)]. Lining synovial cells showed no numerical or morphological change on treatment of with the agonist (400 μg/gel) [Fig. 6(E)], and the histological scoring for inflammation in the treated side was equal to that in the contralateral side [Fig. 6(F)]. These results

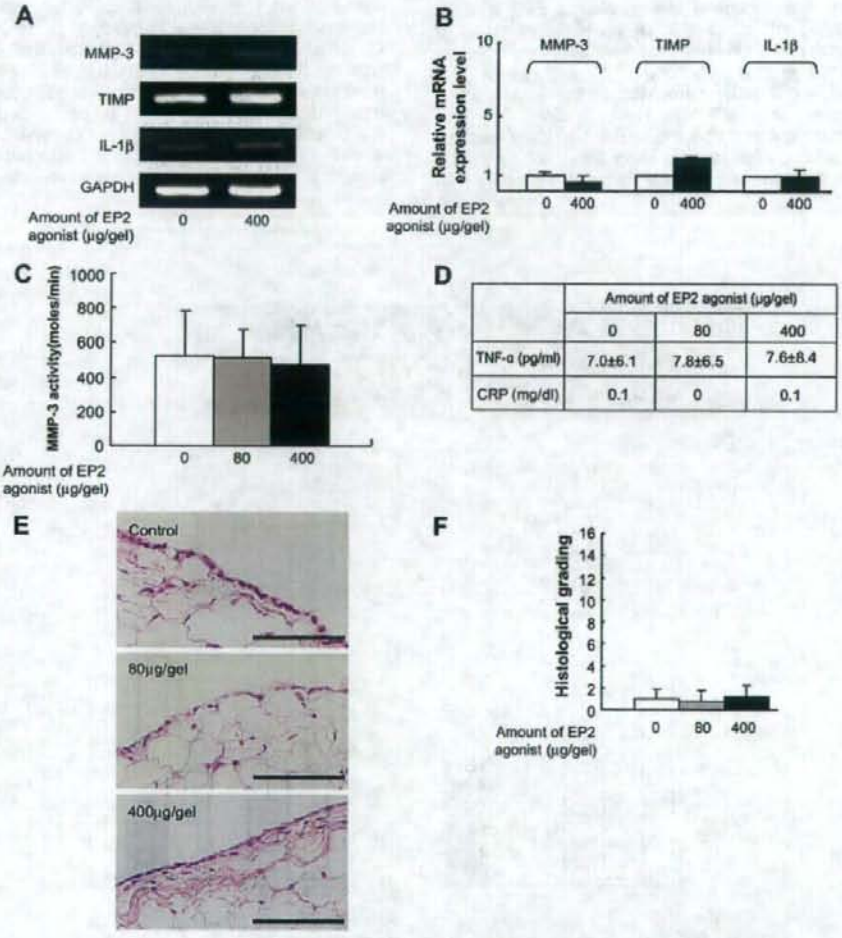

Fig. 6. EP2 agonist did not induce inflammation of the synovium. Inflammatory signs in knee joints were investigated in contralateral or EP2 agonist (80 or 400 μg/gel)-treated samples at 4 weeks after the operation in the osteochondral defect model. A and B: mRNA expression of inflammatory cytokines of cells in the synovium. RNA extracted from synovium was analyzed by semi-quantitative (A) and quantitative (B) RT-PCR. C: Activity of MMP3 in joint fluid. Joint fluid was collected from knee joints of contralateral (open square) and EP2 agonist-treated (blackened square) samples, and the activity of MMP3 was analyzed as described in the Materials and methods section. Five samples were analyzed in each group. D: Amount of TNF-α and CRP in joint fluid. Joint fluid was collected from five knee joints in each group. E: HE staining of synovium in knee joints. Specimens were prepared from a contralateral sample (a), and EP2 agonist-treated samples (b, 80 μg/gel; c, 400 μg/gel). Magnification 200×. Bar = 100 μm. F: Histological scoring of inflammation. Five specimens were analyzed in each of the contralateral and EP2 agonist-treated groups.

indicated that the EP2 agonist induced no significant inflammatory reaction in knee joints at the dose used in this study.

Discussion

PGE2 is a major prostanoid synthesized in response to various stimuli in a variety of cells and exerts local and systemic pleiotropic effects. In general, PGE2 plays a role in maintaining the physiological homeostasis, but in some pathogenic conditions such as inflammation and carcinogenesis, the excess PGE2 induced by factors such as inflammatory cytokines worsens the condition[10]. From this standpoint, PGE2 may be regarded as a pro-inflammatory factor promoting the pathological stage of OA. On the other hand, PGE2 has an anti-inflammatory function. Typical anti-inflammatory actions of PGE2 are demonstrated by the suppressive role of the PGE2 signal *via* EP3 in asthma[20]. As for the PGE2 signal *via* EP2, several reports have analyzed the relationship with inflammation. In human periodontal ligament cells, PGE2 signal *via* EP2/EP4 down-regulated the production of MMP3 and IL-6 stimulated by IL-1[21,22]. An EP4 agonist stimulated the production of MMP9 in macrophages, which was not observed on treatment with an EP2 agonist[23]. The expression of *COX-2* and *MMP9* genes was elevated in macrophages from EP2 null mice[24]. These results suggested that PGE2 acting through EP2 has a minimal role as a pro-inflammatory factor.

Our previous[11] and current study suggested that PGE2 signal *via* EP2 is not only anti-inflammatory but also promotes the regeneration of articular cartilage. The regeneration process of osteochondral defect may mimic the endochondral ossification in fracture healing, and several studies have already shown that the PGE2 signal involved in this process[25–28], among which signals *via* EP2 was particularly important[29]. Cells derived from bone marrow may play a central role in this process. On the other hand, the chondral defect model in this study may mimic the some stage of OA, in which cartilage tissue disappeared and subchondral bone was sclerosed. At this stage, the recruitment of bone marrow-derived cells was minimum, and, therefore, restoration of cartilage tissues was hardly observed. The therapeutic effects of EP2 agonist in this type of model, therefore, may be due to its effects directly on the remaining chondrocytes which are at the resting state in physiological condition as indicated by no PCNA staining [Fig. 3(A)]. The effects of EP2 agonist treatment were more prominent at the later time point (12 weeks) in both chondral and osteochondral defect models, suggesting that the regeneration of cartilage tissue was dependent on the growth of articular chondrocytes with low growth property. We observed that the amount of regenerated tissues was much less at 12 weeks than at 4 weeks after operation in control and contralateral samples, suggesting that regenerated cartilage tissues may lack the proper quality to maintain the structure, and the treatment with EP2 agonist may prevent such degeneration.

One of interesting finding in the current study is that the treatment with EP2 agonist enhanced the reconstruction of boundary between articular cartilage and subchondral bone, which is an important factor to maintain the articular structure. We have no clear explanation for this interesting phenomenon. As mentioned above, EP2 agonists stimulate the growth of both cartilage and bone marrow cells, which may relate to the physiological reconstruction of boundary.

It should be noted that the histological scale of contralateral samples tended to be better than that of control samples (Figs. 1 and 2) and the scales of contralateral samples of 400 μg/gel-treated animals were significantly better than 80 μg/gel-treated animals at 12 weeks [Fig. 2(D), $P = 0.02$], suggesting that there might be an effect from the treated-site through the systemic circulation. Although there were no signs of a general effect of PGE2 such as a reduction in blood pressure (data not shown), continuous release of the EP2 agonist may affect tissue regeneration on the contralateral side.

The ideal regeneration-promoting therapeutics will be small molecules which can be produced in a large amount, promote the regeneration of articular cartilage with a physiological structure, and have no adverse effects in other tissues either locally or systemically. No osteophyte formation was observed in any samples described in this study and also samples observed for a longer period (24 weeks) (data not shown). The results of this study suggested that the EP2 agonist is a promising candidate for such a new drug. Because EP4 is not expressed in normal articular chondrocytes[11], we have been focusing the analysis of EP2 agonist. In the case of osteochondral defect model, however, the combination of EP2/EP4 agonist is a reasonable choice to test considering the fact that the simultaneous activation of EP2 and EP4 cooperatively induced type II collagen mRNA expression[7]. The current experimental model has been used in several prior investigations of various articular repair procedures[30], but may not reflect the pathogenesis of OA (no mechanical factor, no inflammation, no aging factor). Further confirmation of the effect of EP2 agonists in combination with a more effective drug delivery system and experimental OA models in larger animals may lead to a new way to treat OA.

Conflict of interest

The authors declare that they have no conflict of interest.

Acknowledgments

We are grateful to Drs H. Ito, H. Yoshitomi, K. Nishitani, and B. Liang for providing helpful suggestions. This work was supported by Grants-in-aid for Scientific Research from the Japan Society for the Promotion of Science, from the Ministry of Education, Culture, Sports, Science, and Technology, and from the Ministry of Health, Labor, and Welfare.

Supplementary material

Supplementary material for this article may be found, in the online version, at doi: 10.1016/j.joca.2008.09.003.

References

1. Goldring MB, Goldring SR. Osteoarthritis. J Cell Physiol 2007;213: 626–34.
2. Goldring SR, Goldring MB. The role of cytokines in cartilage matrix degeneration in osteoarthritis. Clin Orthop Relat Res 2004;(427 Suppl):S27–36.
3. Martel-Pelletier J, Pelletier JP, Fahmi H. Cyclooxygenase-2 and prostaglandins in articular tissues. Semin Arthritis Rheum 2003;33:155–67.
4. Bunning RA, Russell RG. The effect of tumor necrosis factor alpha and gamma-interferon on the resorption of human articular cartilage and on the production of prostaglandin E and of caseinase activity by human articular chondrocytes. Arthritis Rheum 1989;32:780–4.
5. Miwa M, Saura R, Hirata S, Hayashi Y, Mizuno K, Itoh H. Induction of apoptosis in bovine articular chondrocyte by prostaglandin E(2) through cAMP-dependent pathway. Osteoarthritis Cartilage 2000;8: 17–24.

6. Riquet FB, Lai WF, Birkhead JR, Suen LF, Karsenty G, Goldring MB. Suppression of type I collagen gene expression by prostaglandins in fibroblasts is mediated at the transcriptional level. Mol Med 2000;6:705–19.
7. Miyamoto M, Ito H, Mukai S, Kobayashi T, Yamamoto H, Kobayashi M, *et al.* Simultaneous stimulation of EP2 and EP4 is essential to the effect of prostaglandin E2 in chondrocyte differentiation. Osteoarthritis Cartilage 2003;11:644–52.
8. Di Battista JA, Doré S, Morin N, He Y, Pelletier JP, Martel-Pelletier J. Prostaglandin E2 stimulates insulin-like growth factor binding protein-4 expression and synthesis in cultured human articular chondrocytes: possible mediation by Ca(++)-calmodulin regulated processes. J Cell Biochem 1997;65:408–19.
9. Lowe GN, Fu YH, McDougall S, Polendo R, Williams A, Benya PD, *et al.* Effects of prostaglandins on deoxyribonucleic acid and aggrecan synthesis in the RCJ 3.1C5.18 chondrocyte cell line: role of second messengers. Endocrinology 1996;137:2208–16.
10. Sugimoto Y, Narumiya S. Prostaglandin E receptors. J Biol Chem 2007; 282:11613–7.
11. Aoyama T, Liang B, Okamoto T, Matsusaki T, Nishijo K, Ishibe T, *et al.* PGE2 signal through EP2 promotes the growth of articular chondrocytes. J Bone Miner Res 2005;20:377–89.
12. Tani K, Naganawa A, Ishida A, Egashira H, Sagawa K, Harada H, *et al.* Design and synthesis of a highly selective EP2-receptor agonist. Bioorg Med Chem Lett 2001;11:2025–8.
13. Okada H. One- and three-month release injectable microspheres of the LH–RH superagonist leuprorelin acetate. Adv Drug Deliv Rev 1997; 28:43–70.
14. Katayama R, Wakitani S, Tsumaki N, Morita Y, Matsushita I, Gejo R, *et al.* Repair of articular cartilage defects in rabbits using CDMP1 gene-transfected autologous mesenchymal cells derived from bone marrow. Rheumatology (Oxford) 2004;43:980–5.
15. Yoshimi T, Kikuchi T, Obara T, Yamaguchi T, Sakakibara Y, Itoh H, *et al.* Effects of high-molecular-weight sodium hyaluronate on experimental osteoarthrosis induced by the resection of rabbit anterior cruciate ligament. Clin Orthop Relat Res 1994;298:296–304.
16. Fukuda T, Tani Y, Kobayashi T, Hirayama Y, Hino O. A new Western blotting method using polymer immunocomplexes: detection of Tsc1 and Tsc2 expression in various cultured cell lines. Anal Biochem 2000;285:274–6.
17. Qi C, Changlin H, Zefeng H. Matrix metalloproteinases and inhibitor in knee synovial fluid as cartilage biomarkers in rabbits: the effect of high-intensity jumping exercise. J Surg Res 2007;140:149–57.
18. Wu LD, Yu HC, Xiong Y, Feng J. Effect of dehydroepiandrosterone on cartilage and synovium of knee joints with osteoarthritis in rabbits. Rheumatol Int 2006;27:79–85.
19. Kawashima-Ohya Y, Satakeda H, Kuruta Y, Kawamoto T, Yan W, Akagawa Y, *et al.* Effects of parathyroid hormone (PTH) and PTH-related peptide on expressions of matrix metalloproteinase-2, -3, and -9 in growth plate chondrocyte cultures. Endocrinology 1998;139:2120–7.
20. Kunikata T, Yamane H, Segi E, Matsuoka T, Sugimoto Y, Tanaka S, *et al.* Suppression of allergic inflammation by the prostaglandin E receptor subtype EP3. Nat Immunol 2005;6:524–31.
21. Yan M, Noguchi K, Ruwanpura SM, Ishikawa I. Cyclooxygenase-2-dependent prostaglandin (PG) E2 downregulates matrix metalloproteinase-3 production *via* EP2/EP4 subtypes of PGE2 receptors in human periodontal ligament cells stimulated with interleukin-1alpha. J Periodontol 2005;76:929–35.
22. Noguchi K, Maeda M, Ruwanpura SM, Ishikawa I. Prostaglandin E2 (PGE2) downregulates interleukin (IL)-1alpha-induced IL-6 production *via* EP2/EP4 subtypes of PGE2 receptors in human periodontal ligament cells. Oral Dis 2005;11:157–62.
23. Tchetina EV, Di Battista JA, Zukor DJ, Antoniou J, Poole AR. Prostaglandin PGE2 at very low concentrations suppresses collagen cleavage in cultured human osteoarthritic articular cartilage: this involves a decrease in expression of proinflammatory genes, collagenases and COL10A1, a gene linked to chondrocyte hypertrophy. Arthritis Res Ther 2007;9:R75.
24. Pavlovic S, Du B, Sakamoto K, Khan KM, Natarajan C, Breyer RM, *et al.* Targeting prostaglandin E2 receptors as an alternative strategy to block cyclooxygenase-2-dependent extracellular matrix-induced matrix metalloproteinase-9 expression by macrophages. J Biol Chem 2006;281:3321–8.
25. Simon AM, Manigrasso MB, O'Connor JP. Cyclo-oxygenase 2 function is essential for bone fracture healing. J Bone Miner Res 2002;17: 963–76.
26. Gerstenfeld LC, Al-Ghawas M, Alkhiary YM, Cullinane DM, Krall EA, Fitch JL, *et al.* Selective and nonselective cyclooxygenase-2 inhibitors and experimental fracture-healing. Reversibility of effects after short-term treatment. J Bone Joint Surg Am 2007;89:114–25.
27. Einhorn TA. The science of fracture healing. J Orthop Trauma 2005; 19(10 Suppl):S4–6.
28. Yamakawa K, Kamekura S, Kawamura N, Saegusa M, Kamei D, Murakami M, *et al.* Association of microsomal prostaglandin E synthase 1 deficiency with impaired fracture healing, but not with bone loss or osteoarthritis, in mouse models of skeletal disorders. Arthritis Rheum 2008;58:172–83.
29. Paralkar VM, Borovecki F, Ke HZ, Cameron KO, Lefker B, Grasser WA, *et al.* An EP2 receptor-selective prostaglandin E2 agonist induces bone healing. Proc Natl Acad Sci U S A 2003; 100:6736–40.
30. Breinan HA, Hsu HP, Spector M. Chondral defects in animal models: effects of selected repair procedures in canines. Clin Orthop Relat Res 2001;(391 Suppl):S219–30.